Computational and Applied Mathematics Journal
2018; 4(2): 31-42
http://www.aascit.org/journal/camj
ISSN: 2381-1218 (Print); ISSN: 2381-1226 (Online)

American Association for Science and Technology

Squeezing Unsteady MHD Cu-water Nanofluid Flow Between Two Parallel Plates in Porous Medium with Suction/Injection

Alok Kumar Pandey*, Manoj Kumar

Department of Mathematics, Statistics and Computer Science, Govind Ballabh Pant University of Agriculture and Technology, Pantnagar, India

Email address

mr.alokpandey1@gmail.com (A. K. Pandey), mnj_kumar2004@yahoo.com (M. Kumar)

*Corresponding author

Citation

Alok Kumar Pandey, Manoj Kumar. Squeezing Unsteady MHD Cu-water Nanofluid Flow Between Two Parallel Plates in Porous Medium with Suction/Injection. *Computational and Applied Mathematics Journal.* Vol. 4, No. 2, 2018, pp. 31-42.

Received: January 11, 2018; **Accepted**: January 29, 2018; **Published**: March 2, 2018

Abstract: In this article the influence of suction/injection on flow and heat transfer in squeezing unsteady magneto-hydrodynamics flow between parallel plates in porous medium in the presence of thermal radiation for Cu-water nanofluid has been analyzed. The radiative heat flux is used to portray energy equation by using Rosseland approximation. The set of altered ODEs with appropriate boundary conditions have been solved numerically by applying shooting method along with Runge-Kutta-Fehlberg 4-5th order of integration technique. The influences of relatable parameters on dimensionless flow field and thermal field have been shown in graphs and tabular form. The results elucidate that heat transfer coefficient decreases as increasing in thermal radiation parameter while the absolute values of coefficient of skin friction enhances with amplify in magnetic field parameter. The outcomes also declared that as enhance in the values of suction/injection parameter both the velocity and temperature profiles regularly decline.

Keywords: MHD, Nanofluid, Porous Medium, Suction/Injection, Thermal Radiation

1. Introduction

Analysis of heat and mass transfer enhanced during last few decade due to large application in several branches of science and engineering. Evaporation water from tarn to the environment, blood sanitization inside the kidneys and liver are few applications of mass transfer, and heat transfer entail in the field of condensers and evaporators. The heat and mass transfer rate entail in unsteady squeezing glutinous flow field has lot of use in lubrication method, chemical dispensation equipment, polymer dispensation, spoil of crops due to frosty, fog formation and dispersion. Azimin and Riazi [1] analyzed the impact of heat transfer between two analogous disks for GO-water nanofluid. They found that volume concentration of nanoparticle increases on increasing the values of Brownian number. Aziz et al. [2] have discussed the effect of free convection on nanofluid past a smooth plane plate implanted in porous medium and in the happening of gyrotactic microorganisms. They found that on increasing the value of bio-convection parameters Nusselt number, rate of mass transfer and motile density parameter enhanced while decreases on increasing the values of buoyancy parameter *Nr*. Das et al. [3] have examined the influence of entropy exploration on MHD flow during a vertical porous channel via convective heat source for nanofluid. Domairry and Hatami [4] have discussed numerical investigation of Squeezing flowthrough similar plates with Cu–water nanofluid. They projected that on raising the values of volume fraction of solid particle, there is no change in velocity boundary layer depth. Fakour et al. [5] deliberated the effect of magnetohydrodynamic and heat conduction of a nanofluids flow through a channel with porous walls. Grosan et al. [6] considered the free convection effect of heat transfer within a square cavity packed through a porous medium in nanofluids. Gupta and Ray [7] have studied numerical analysis of the squeezing nanofluid flow among two analogous plates. They found that as increase in Prandtl number and Eckert number, temperature of the nanoparticle increases. Jha et al. [8] analyzed the effect of natural convection flow inside an upright similar plate. They found that on increasing in the outcome of rarefaction and fluid wall interaction, volume flow rate increases, while it reduces on enhancing the values of Hartmann number. Khalid et al. [9] purposed the free convection effect of MHD flow of past above an oscillating perpendicular plate entrenched in a porous medium for casson fluid. Kuznetsov and Nield [10] investigated the impact of natural convective flow inside a porous medium in nanofluids for Cheng-Minkowycz problem for: A revised model. They found that decreased Nusselt number is free of the values of Brownian number when on the boundary zero nanoparticle flux imposed. Mustafa et al. [11] have introduced the impact of heat and mass rate within squeezing unsteady nanofluid flow along with corresponding plates. Pourmehran et al. [12] analyzed the squeezing unsteady flow through two infinite parallel plates for nanofluid by analytical methods. They scrutinized that on increasing the values Nusselt number volume fraction of nanoparticle enhances, while on enhancing the values of Eckert number, the values of squeeze number decreases. Sheikholeslami and Ganji [13] discussed the effect of nanofluids flow and rate of heat transfer between analogous plates in the presence of Brownian motion using differential transformation method. They explained that Nusselt number is escalating with volume fraction of nanoparticle while Hartmann number and heat source parameter are decreasing function with squeeze number. Wubshet and Shankar [14] premeditated the influence of MHD as well as heat transfer over a stretching surface in the existence of thermal radiation and slip conditions with nanofluid. They found that on enhancing the values of magnetic parameter velocity of nanofluid reduces and temperature of the surface decreases on enhancing the values of Prandtl number. Lately, Pandey and Kumar [15] have proposed the influence of suction/injection and slip on MHD nanofluid flow due to a porous wedge in continuation of viscous dissipation and convective boundary conditions. Once again, Pandey and Kumar [16] demonstrated the influence of natural convection and thermal radiation on nanofluid flow due to a stretching cylinder in the occurrence of porous medium, viscous dissipation and slip boundary conditions. Hatami et al. [17] have been applied the optimal collection method (OCM) to obtained the results of forced convective Al_2O_3-nanofluid flow over a plate vertical plate by utilized variable magnetic field. The control volume finite element method is taken by [18] to find the outcomes to MHD forced convective Fe_3O_4-water nanofluid flow in a semi annulus enclosure. Mahmoudi et al. [19] have used Lattice Boltzmann method (LBM) is employed to found the results to heat transfer and nanofluid flow in an open cavity. MHD flow and heat transfer analysis on nanofluid flow between parallel plates with Duan-Rach approach (DRA) was studied by [20]. The different approaches have been applied to acquire the results to nanofluid flow over a stretching/shrinking surface [21-24]. The nanofluid flow and heat transfer in a micro-channel is investigated by Karimipour et al. [25]. Behrangzade and Heyhat [26] examined the thermo and hydrodynamic features of Ag-water nanofluid by designing an experimental rig. Hayat et al. [27] have been employed homotopy analysis method (HAM) to find the solutions to nanofluid flow due to convectively heated Riga plate. Ahmadi et al. [28] considered influence of heat transfer nanofluid flow due to a stretching flat plate using Differential Transformation Method (DTM). Recently, MHD micropolar nanofluid flow between parallel plates was studied by Rashidi et al. [29]. Sheikholeslami and Ganji [30] have analyzed the heat transfer influence of Cu-water nanofluid flow between two parallel plates utilizing homotopy perturbation method (HPM). Later on, the studied of heat transfer analysis of steady nanofluid flow between parallel plates is analyzed with the help of DTM is given by [31]. Ganga et al. [32] have utilized the homotopy analysis method to examine the influence of heat generation/absorption and viscous-Ohmic dissipation on nanofluid flow over a vertical plate. Zin et al. [33] have investigated the influence of MHD free convective flow of nanofluid over an oscillating vertical plate due to porous medium. They proposed the Laplace transform technique to solve the principal equations. The implicit finite difference method has been used to study the influence of heat generation and natural convection in an inclined porous triangular enclosure filled with nanofluid by Mansour and Ahmed [34].

The aspire of the current analysis is to study the impact of thermal radiation and suction/injection on squeezing unsteady MHD Cu-water nanofluids flow between analogous plates in the existence of porous medium. The equations that obtained have been cracked with the help of shooting method via 4-5th Runge-Kutta-Fehlberg technique. The impact of different objective parameters on the velocity and temperature are depicted graphically and analyzed.

2. Mathematical Formulation

Assumed a two dimensional unsteady squeezing MHD nanofluid flow between two analogous plates in porous medium, in the existence of the thermal radiation and suction/injection. An oblique magnetic field with variable strength B_0 acts normal to the plates. The space between two plates is $z = \pm l\left(1-\alpha t\right)^{0.5} = \pm h\left(t\right)$. For $\alpha > 0$, the both plate are squashed until they contact $t = \dfrac{1}{\alpha}$ and for $\alpha < 0$, the two plate are take apart. The effect of viscous dissipation is also considered and it occurs at large values of Eckert number $\left(Ec >> 1\right)$. Copper (Cu) nanofluid is based on regular fluid (water) with assertions that incompressible, no chemical reaction, solid particle (Cu) and the regular fluid (water) are in equilibrium. Motion of the nanofluid considered as laminar and stable. The graphical mold of the physical model has been specified along with flow pattern and coordinate system in Figure 1.

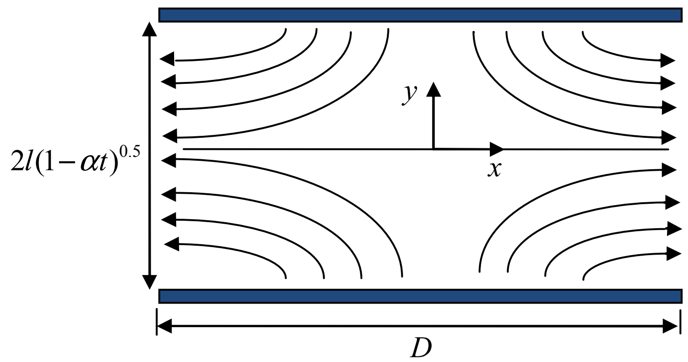

Figure 1. *Flow configuration and coordinate system.*

The essential equations of mass, momentum and heat transfer for nanofluid are expressed as [4]:

$$\frac{\partial u}{\partial x}+\frac{\partial v}{\partial y}=0 \tag{1}$$

$$\rho_{nf}\left(\frac{\partial u}{\partial t}+u\frac{\partial u}{\partial x}+v\frac{\partial u}{\partial y}\right)=-\frac{\partial p}{\partial x}+\mu_{nf}\left(\frac{\partial^2 u}{\partial x^2}+\frac{\partial^2 u}{\partial y^2}\right)-\frac{\nu\rho_{nf}}{k_1}u-\sigma B_0^2 u \tag{2}$$

$$\rho_{nf}\left(\frac{\partial v}{\partial t}+u\frac{\partial v}{\partial x}+v\frac{\partial v}{\partial y}\right)=-\frac{\partial p}{\partial y}+\mu_{nf}\left(\frac{\partial^2 v}{\partial x^2}+\frac{\partial^2 v}{\partial y^2}\right)-\frac{\nu\rho_{nf}}{k_1}v-\sigma B_0^2 v \tag{3}$$

$$\frac{\partial T}{\partial t}+u\frac{\partial T}{\partial x}+v\frac{\partial T}{\partial y}=\frac{k_{nf}}{\left(\rho C_p\right)_{nf}}\left(\frac{\partial^2 T}{\partial x^2}+\frac{\partial^2 T}{\partial y^2}\right)+\frac{\mu_{nf}}{\left(\rho C_p\right)_{nf}}\left(4\left(\frac{\partial u}{\partial x}\right)^2+\left(\frac{\partial u}{\partial y}+\frac{\partial v}{\partial x}\right)^2\right)-\frac{1}{\left(\rho C_p\right)_{nf}}\frac{\partial q_r}{\partial y} \tag{4}$$

Using Rosseland's approximation (see in Ref. [14]), The heat flux for radiation defined as:

$$q_r=-\frac{4\sigma^*}{3k^*}\frac{\partial T^4}{\partial y} \tag{5}$$

where $\left(\sigma^*, k^*\right)$ locates the Stefan–Boltzmann constant and coefficient of mean absorption respectively. We suppose that the temperature deviation inside the flow is to facilitate T^4 extended in a Taylor's series and growing T^4 about T_∞ and deserting terms of higher order. We acquire:

$$T^4 \cong 4T_\infty^3 T-3T_\infty^4 \tag{6}$$

By means of equations (5) and (6), equation (4) turns into:

$$\frac{\partial T}{\partial t}+u\frac{\partial T}{\partial x}+v\frac{\partial T}{\partial y}=\frac{k_{nf}}{\left(\rho C_p\right)_{nf}}\frac{\partial^2 T}{\partial x^2}+\frac{k_{nf}}{\left(\rho C_p\right)_{nf}}\left(1+\frac{16\sigma * T_\infty^3}{3k^* k_{nf}}\right)\frac{\partial^2 T}{\partial y^2}+\frac{\mu_{nf}}{\left(\rho C_p\right)_{nf}}\left(4\left(\frac{\partial u}{\partial x}\right)^2+\left(\frac{\partial u}{\partial y}+\frac{\partial v}{\partial x}\right)^2\right) \tag{7}$$

The coupled boundary conditions are:

$$u=0\,,\ v=V_w\left(x,t\right)=\frac{dh}{dt}\,,\ T=T_H \text{ at } y=h\left(t\right)\ \frac{\partial u}{\partial y}=0\,,\ v=-\frac{\alpha l}{2\left(1-\alpha t\right)^{0.5}}f_w\,,\ \frac{\partial T}{\partial y}=0 \text{ at } y=0\,. \tag{8}$$

Now, f_w stand for suction parameter if $\left(f_w>0\right)$ and for injection parameter $\left(f_w<0\right)$. Again, along x and y direction velocity components are $\left(u, v\right)$ correspondingly. Further μ_{nf} be the effective dynamic viscosity, ρ_{nf} be the effective density, $\left(\rho C_p\right)_{nf}$ be the effective heat capacity and k_{nf} be the effective thermal conductivity of nanofluid and written as [4, 35]:

$$\begin{cases} \rho_{nf} = (1-\varphi)\rho_f + \varphi\rho_s, (\rho C_p)_{nf} = (1-\varphi)(\rho C_p)_f + \varphi(\rho C_p)_s, \\ \mu_{nf} = \dfrac{\mu_f}{(1-\varphi)^{2.5}}, \dfrac{k_{nf}}{k_f} = \dfrac{k_s + 2k_f - 2\varphi(k_f - k_s)}{k_s + 2k_f + 2\varphi(k_f - k_s)} \end{cases} \tag{9}$$

where ϕ be the solid volume fraction furthermore the subscripts f and s denote the regular fluid (water) and solid particle, respectively. The thermophysical properties of regular fluid (water) and solid particle (Cu) are displayed in Table 1.

Table 1. *Thermo physical properties of Cu-water nanofluid as in [4].*

	ρ (kg/m^3)	C_p (j/kg K)	k (W/m K)
Pure water	997.1	4179	0.613
Copper (Cu)	8933	385	401

Equations (2), (3) and (7) can be distorted into non-linear ODEs by using the following similarity variables (see also Ref. [4]):

$$\eta = \frac{y}{l(1-\alpha t)^{\frac{1}{2}}},\ u = \frac{\alpha x}{2(1-\alpha t)} f'(\eta),\ v = -\frac{\alpha l}{2(1-\alpha t)^{\frac{1}{2}}} f(\eta),\ \theta = \frac{T}{T_H} \tag{10}$$

The altered ODEs are:

$$f'''' - SA_1(1-\varphi)^{2.5}(\eta f''' + 3f'' + f'f'' - ff''') - (\gamma + M)f'' = 0 \tag{11}$$

$$(1+Nr)\theta'' + \Pr S\left(\frac{A_2}{A_3}\right)(\theta' f - \eta\theta') + \frac{\Pr Ec}{A_3(1-\varphi)^{2.5}}\left[f''^2 + 4\delta^2 f'^2\right] = 0 \tag{12}$$

The boundary conditions (8) become:

$$\begin{cases} f(0) = f_w,\ f''(0) = 0,\ \theta'(0) = 1\ at\ \eta = 0 \\ f(1) = 1,\ f'(1) = 0,\ \theta(1) = 1\ as\ \eta = 1 \end{cases} \tag{13}$$

where $S = \dfrac{\alpha l^2}{2\nu_f}$ be the Squeeze number, $Ec = \dfrac{\rho_f}{(\rho C_p)_f}\left(\dfrac{\alpha x}{2(1-\alpha t)}\right)^2$ be the Eckert number, $\Pr = \dfrac{\mu_f(\rho C_p)_f}{\rho_f k_f}$ be the Prandtl number, $Nr = \dfrac{16T_\infty^3\sigma^*}{3k_{nf}k^*}$ be the thermal radiation parameter, $\gamma = \dfrac{2l^2\nu(1-\alpha t)}{k_1\mu_{nf}}$ be the porous medium parameter, $M = \dfrac{2\sigma B_0^2 l^2(1-\alpha t)}{\rho_f\mu_{nf}}$ the magnetic parameter, $f_w = -\dfrac{2(1-\alpha t)^{1/2}V_w(x)}{\alpha l}$ be the suction/injection parameter, $\delta = \dfrac{l}{x}$ be the reference length and the constants A_1, A_2 and A_3 are defined as:

$$A_1 = (1-\varphi) + \varphi\frac{\rho_s}{\rho_f},\ A_2 = (1-\varphi) + \varphi\frac{(\rho C_p)_s}{(\rho C_p)_f},\ A_3 = \frac{k_{nf}}{k_f} = \frac{k_s + 2k_f - 2\varphi(k_f - k_s)}{k_s + 2k_f + 2\varphi(k_f - k_s)}. \tag{14}$$

For the practical interest, the coefficient of skin friction C_f and Nusselt number Nu are expressed as:

$$C_f = \frac{\mu_{nf}\left(\dfrac{\partial u}{\partial y}\right)_{y=h(t)}}{\rho_{nf}v_w^2},\ Nu = \frac{lk_{nf}\left(\dfrac{\partial T}{\partial y}\right)_{y=h(t)}}{kT_H} \tag{15}$$

Therefore, the reduced skin friction coefficient C_f^* and reduced Nusselt number Nu^* are written as:

$$C^*_f = \frac{l^2}{x^2(1-\alpha t)\,\mathrm{Re}_x\, C_f} = A_1(1-\phi)^{2.5} f''(1),\ Nu^* = \sqrt{1-\alpha t}\, Nu = -A_3\left(1+Nr\right)\theta'(1) \tag{16}$$

3. Numerical Method

The non-dimensional momentum equation (11) and energy equation (12) jointly with assisting boundary conditions (13) have been tackled numerically through shooting procedure with RKF 4-5th order of integration formula. For this plan, we first changed the obtained primary differential equations in the form of first order ODEs. Let us consider $y_1 = \eta$, $y_2 = f$, $y_3 = f'$, $y_4 = f''$, $y_5 = f'''$, $y_6 = \theta$, $y_7 = \theta'$.

Now the succeeding first order system obtained:

$$\begin{pmatrix} y_1' \\ y_2' \\ y_3' \\ y_4' \\ y_5' \\ y_6' \\ y_7' \end{pmatrix} = \begin{pmatrix} 1 \\ y_3 \\ y_4 \\ y_5 \\ SA_1\left(1-\varphi\right)^{2.5}\left(y_1y_5 + 3y_4 + y_3y_4 - y_2y_5\right) + \left(\gamma + M\right)y_4 \\ y_7 \\ \dfrac{-\Pr S\left(\dfrac{A_2}{A_3}\right)\left(y_7y_2 - y_1y_7\right) - \dfrac{\Pr Ec}{A_3\left(1-\varphi\right)^{2.5}}\left[y_4^2 + 4\delta^2 y_3^2\right]}{1+Nr} \end{pmatrix} \tag{17}$$

and subsequent initial conditions.

$$\begin{pmatrix} y_1 \\ y_2 \\ y_3 \\ y_4 \\ y_5 \\ y_6 \\ y_7 \end{pmatrix} = \begin{pmatrix} 0 \\ f_w \\ p_1 \\ 0 \\ p_2 \\ p_3 \\ 1 \end{pmatrix} \tag{18}$$

The system of first order ODEs (17) via initial conditions (18) is solved using order of fourth-fifth RKF-integration process and appropriate values of unknown initial conditions p_1, p_2 and p_3 are preferred and then numerical integration is applied. Here we contrast the computed values of $f(\eta)$, $f'(\eta)$ and $\theta(\eta)$ as $\eta = 1$, through the specified boundary condition $f(1) = 1$, $f'(1) = 0$ and $\theta(1) = 0$, and regulate the expected values of p_1, p_2 and p_3 to achieve a enhanced approximation for result. The unfamiliar p_1, p_2 and p_3 have been approximated by Newton's scheme such a way that boundary conditions well-matched at highest numerical values of $\eta = 1$ with error less than 10^{-8}.

4. Results and Discussion

The transformed equations (11) and (12) related to the assisting boundary conditions (13) are solved numerically by the aid of fourth-fifth order of Runge-Kutta-Fehlberg approach via shooting procedure. In this study, we analyzed the influence of numerous pertinent parameter such as magnetic field parameter M, porous medium parameter γ, suction/injection parameter f_w, thermal radiation parameter Nr, and nanoparticle volume fraction ϕ on $f'(\eta)$ and $\theta(\eta)$. To authenticate the numerical results obtained, we have compared our results of $f(\eta)$ and $\theta(\eta)$ for divergent values of similarity variable η with Domairry and Hatami [4] as revealed in Table 2 and are found with admirable agreement.

Table 2. *Comparison of the values of $f(\eta)$ and $\theta(\eta)$ for Cu-water when $S = 0.1$, $\Pr = 6.2$, $\delta = 0.1$, $\phi = 0.01$, $Ec = 0.05$ and $Nr = M = \gamma = f_w = 0$ with Domairry and Hatami [4].*

η	**Domairry and Hatami [4]**		**Present Result**	
	$f(\eta)$	$\theta(\eta)$	$f(\eta)$	$\theta(\eta)$
0	0	1.2293076	0	1.2291594
0.1	0.148563042	1.2291512	0.14856868065	1.22900299
0.2	0.294239491	1.2284338	0.29425066529	1.228285490
0.3	0.434130652	1.2264082	0.43414714648	1.226260015
0.4	0.565313773	1.2218221	0.56533526406	1.221674390
0.5	0.684830361	1.2129029	0.68485641383	1.212757234

η	Domairry and Hatami [4]		Present Result	
	$f(\eta)$	$\theta(\eta)$	$f(\eta)$	$\theta(\eta)$
0.6	0.789674916	1.1973334	0.78970498169	1.197192865
0.7	0.876784230	1.1722092	0.87681764517	1.172079151
0.8	0.943027415	1.1339720	0.94306339814	1.133860380
0.9	0.985196818	1.0783086	0.98523446519	1.078224467
1	1.000000000	1.0000000	1.00003828743	0.999950086

Furthermore, Table 3 depicts that the assessment of Nusselt number for the diverse values of Prandtl number Pr and Eckert number Ec in the non-existence of $Nr = 0 = M = f_w = \gamma$, which shows an terrific agreement.

Table 3. *Comparison of the values of Nusselt number* $-\theta'(1)$ *for Copper (Cu) when* $S = 0.5,\ \delta = 0.1,\ Nr = M = \gamma = f_w = 0$ *and* $\phi = 0$.

Pr	Ec	Mustafa et al. [11]	Gupta and Ray [7]	Pourmehran et al. [12]	Present result
0.5	1	1.522368	1.52236745096	1.518859607	1.522519415055
1	1	3.026324	3.02632345997	3.019545607	3.026624241488
2	1	5.98053	5.98052980356	5.967887511	5.981119280239
5	1	14.43941	14.4394056608	14.41394678	14.44079827878
1	0.5	1.513162	1.51316172998	1.509772834	1.513312120744
1	1.2	3.631588	3.63158815197	3.623454726	3.631949089786
1	2	6.051647	6.05264691996	6.039091204	6.0532484829767
1	5	15.13162	15.1316172998	15.09772808	15.133121207441

The scenarios of leading physical parameters on the velocity and temperature profiles are depicted in Figures 2-10. Figures 2 and 3 exhibit that the impact of magnetic field parameter M on velocity and temperature sketches for $Nr = \gamma = 2,\ f_w = 0.5,\ \Pr = 6.2$ and $\phi = 0.02$. The variation in velocity profiles due to several values of M is depicted in Figure 2, the graph cleared that velocity near the wall of range $[0, 0.5)$ reduces with increase in M. However, velocity accelerates in the region of $0.5 < \eta \le 1$. Figure 3 clears that thermal field decelerates close to the vicinity of the surface of plate, while far away from the wall of the plate it enhances. The values of flow rate and Nusselt number are shown in Table 4 for special values of Nr, γ, M, f_w and ϕ. It is obvious from Table 4 that as enlarge in the values of volume fraction of nanoparticle, the absolute value of shear stress rate and coefficient of heat transfer are reduced.

Table 4. *Values of skin friction coefficient* $f''(1)$ *and Nusselt number* $-\theta'(1)$ *for Copper (Cu) when* $Ec = 0.01,\ \Pr = 6.2,\ S = 1$ *and* $\delta = 0.01$.

Nr	γ	M	f_w	φ	$\lvert -f''(1) \rvert$	$-\theta'(1)$
0	2	2	0.5	0.02	2.0920945932	0.0429558322
1						0.0225323966
2						0.0152854158
4	2	2	0.5		2.0920945932	0.0093053391
2	0	2	0.5		1.9438901694	0.0148647313
	1				2.0190028272	0.0150649197
	2				2.0920945932	0.0152854158
2	4	2	0.5		2.2306798552	0.0157224369
2	2	0	0.5		1.9440334782	0.0148669456
		1			2.0194087546	0.0150707413
		2			2.0920945932	0.0152815888
		4			2.2303732505	0.0157181238
2	2	8	0.5		2.4836742559	0.0166195833
2	2	2	-0.7		7.5702584636	0.1869261692
			-0.5		6.6133062839	0.1442129744
			-0.2		5.2103729244	0.0910199088
			0.2		3.4014181890	0.0396874828
2	2	2	0.5	0.02	2.0920945932	0.0152815888
				0.01	2.0826698103	0.0154514421
				0.04	2.1095910317	0.0149568162
2	2	2	0.5	0.06	2.1241401910	0.0146309534

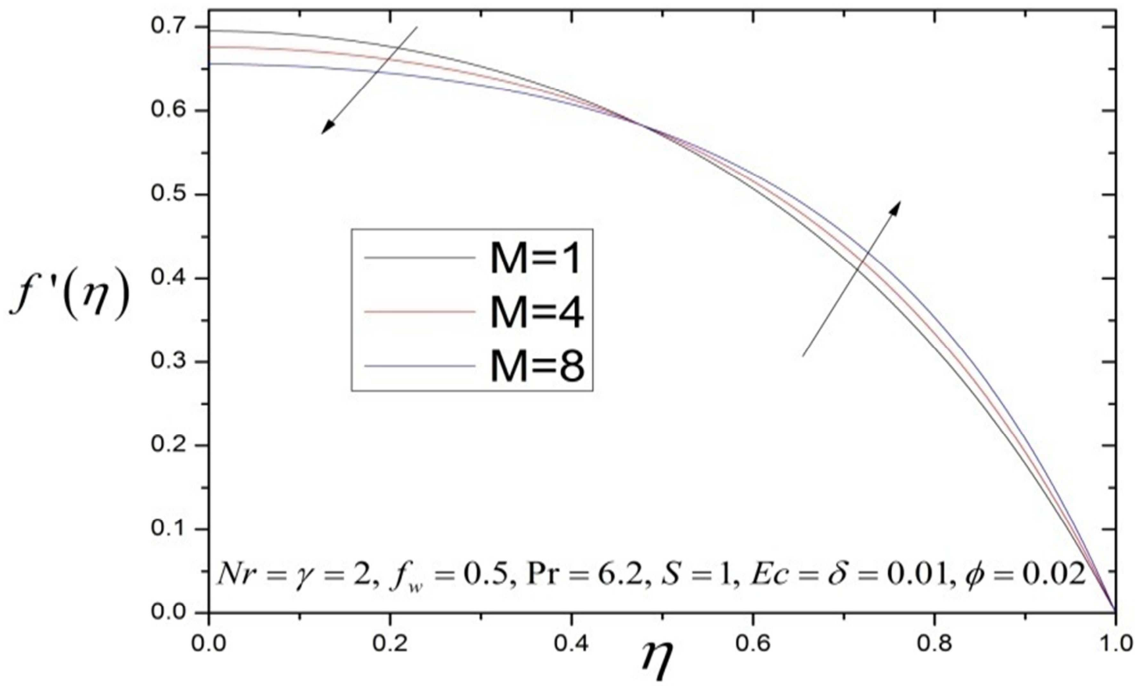

Figure 2. *Variation in velocity f'(η) due to several values of M.*

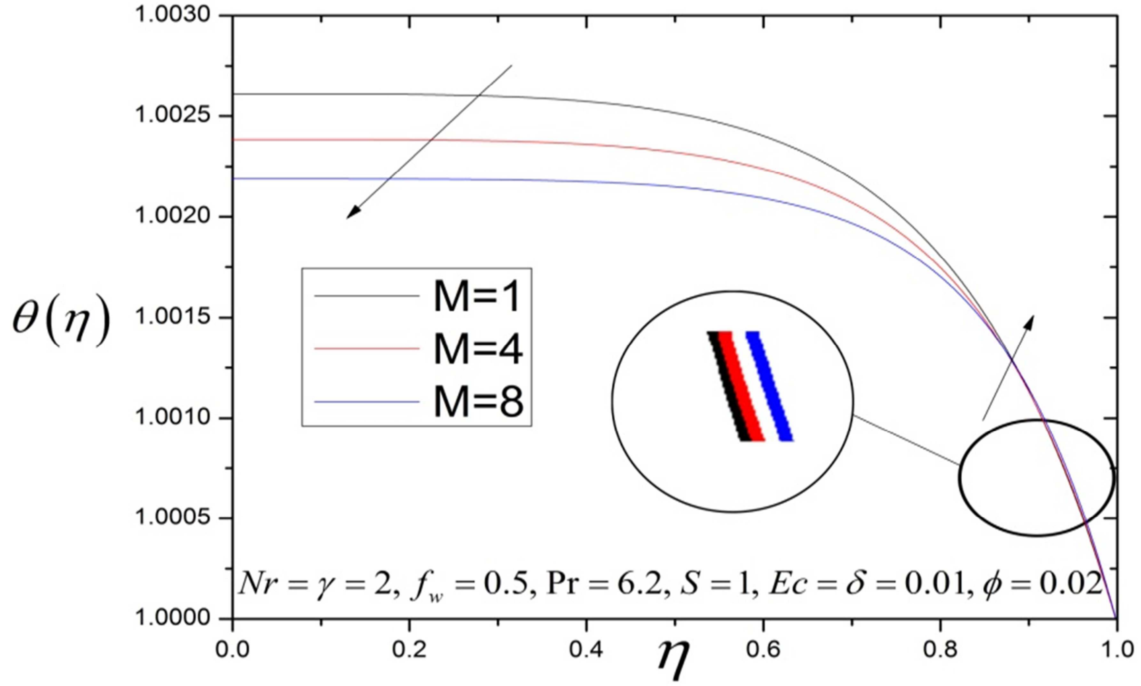

Figure 3. *Variation in temperature θ(η) due to several values of M.*

The flow field and thermal field are affected by the porous medium parameter γ as looking at Figures 4 and 5, respectively. In Figure 4, initially momentum boundary layer width raise along with γ, after then its behavior changed due to away from the wall of plate. Moreover, in Figure 5 temperature curves of Cu-water nanofluid continuously depreciates with amplified in the values of γ, in the region of $0 \le \eta \le 1$ also we observed the behavior of skin friction and Nusselt number from the Table 4, in other words we can say that the heat transfer rate and magnitude of skin friction coefficient are amplified with γ. The temperature profiles of nanofluid are influenced by thermal radiation parameter Nr for the fixed values of governing parameters as such $M = 2 = \gamma$, $\Pr = 6.2$, $f_w = 0.5$, $Ec = 0.01 = \delta$, $S = 1$ and $\phi = 0.02$, is revealed in Figure 6. It is evident from this curves that thermal field frequently decelerates with augmentation in Nr for every values of η. Moreover, thermal boundary layer width also diminishes as raised the radiation parameter. Furthermore, Table 4 indicates that the heat transfer coefficient continuously decreases.

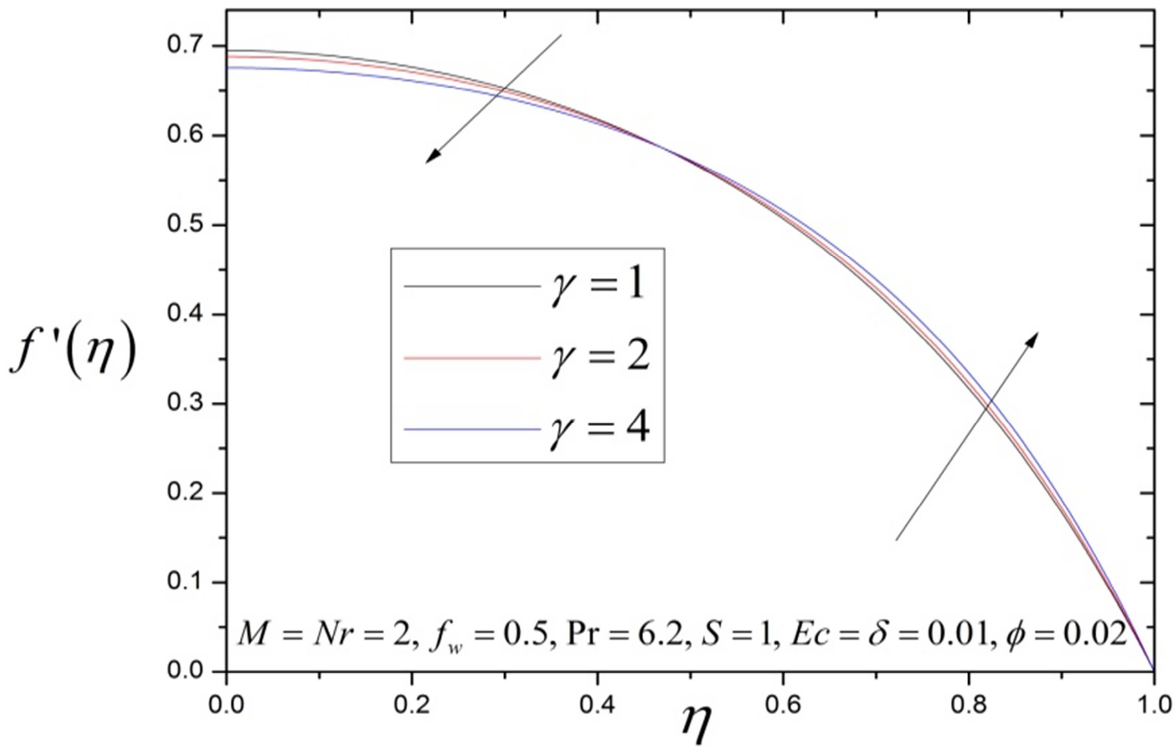

Figure 4. *Variation in velocity f'(η) due to several values of γ.*

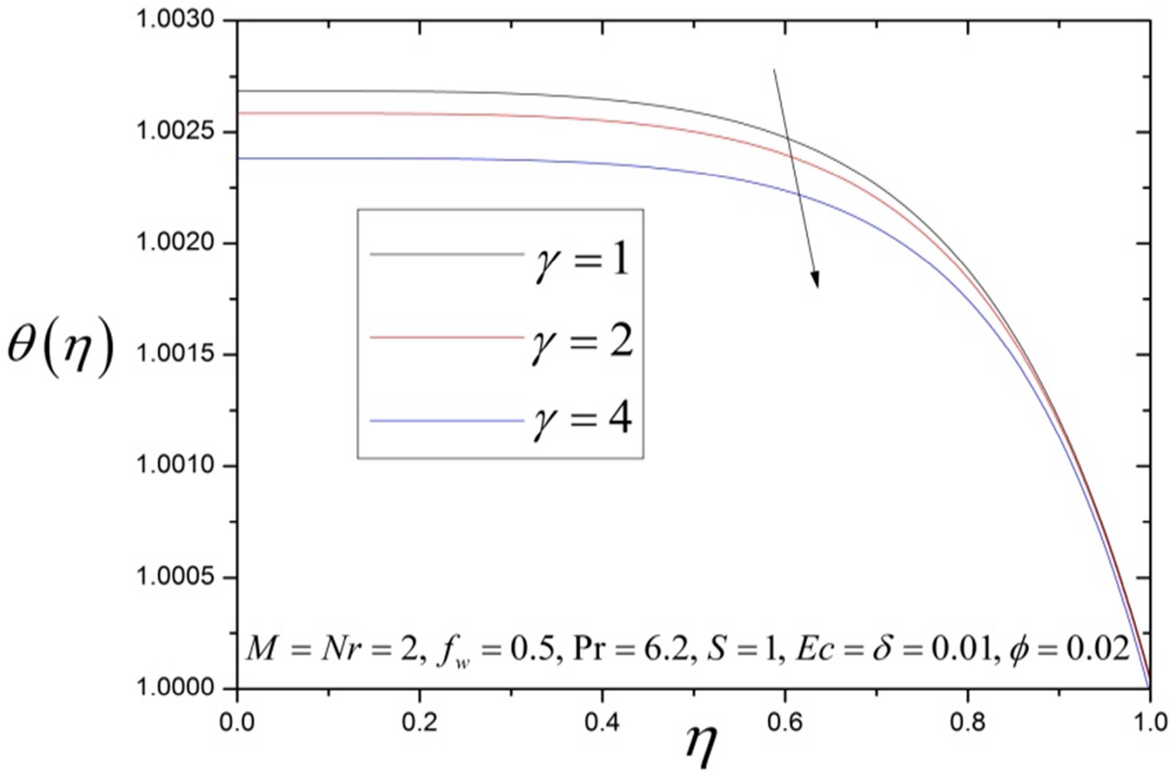

Figure 5. *Variation in temperature θ(η) due to several values of γ.*

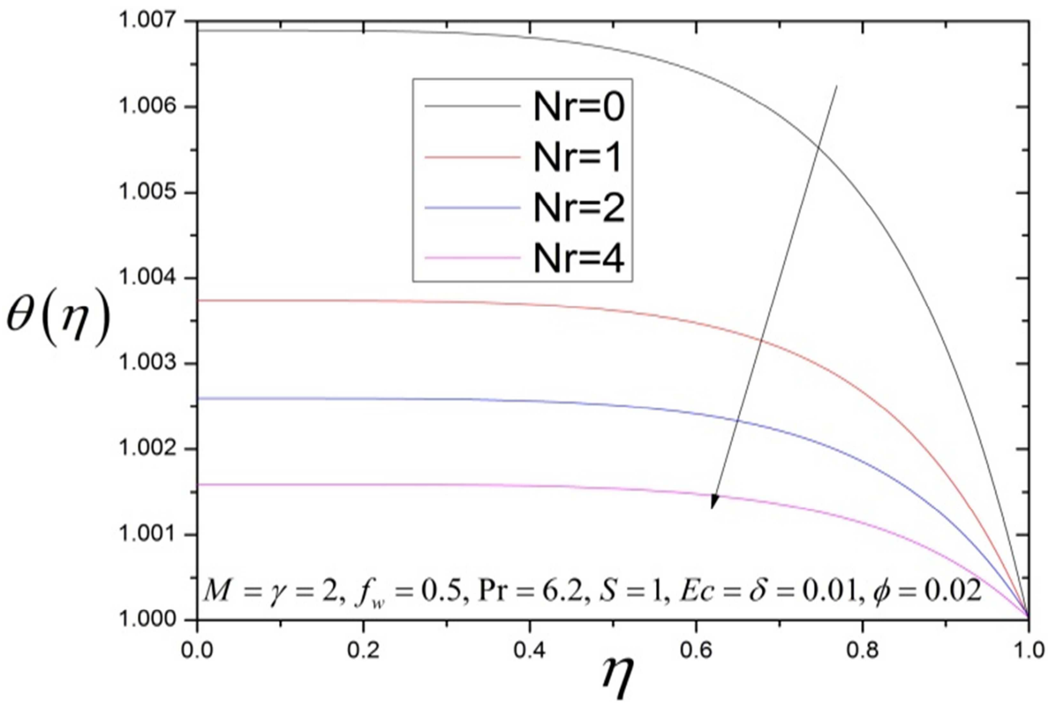

Figure 6. *Variation in temperature θ(η) due to several values of Nr.*

The change in velocity and temperature graphs due to dimensionless suction/injection parameter f_w are exhibited in Figures 7 and 8, correspondingly. On focusing Figure 7, we observed that flow field of nanofluid decreases as accelerate in the values of f_w, in the specified domain $[0,1]$. The change in absolute value of skin friction $|-f''(0)|$ and Nusselt number $-\theta'(0)$ corresponding to suction/injection parameter is shown in Table 4. On looking at this table we noticed that the values of $|-f''(0)|$ and $-\theta'(0)$ are reduced with enhance in f_w. Similarly, Figure 8 shows that thermal field reduces as increase in suction/blowing parameter in the range of $0 \le \eta \le 1$.

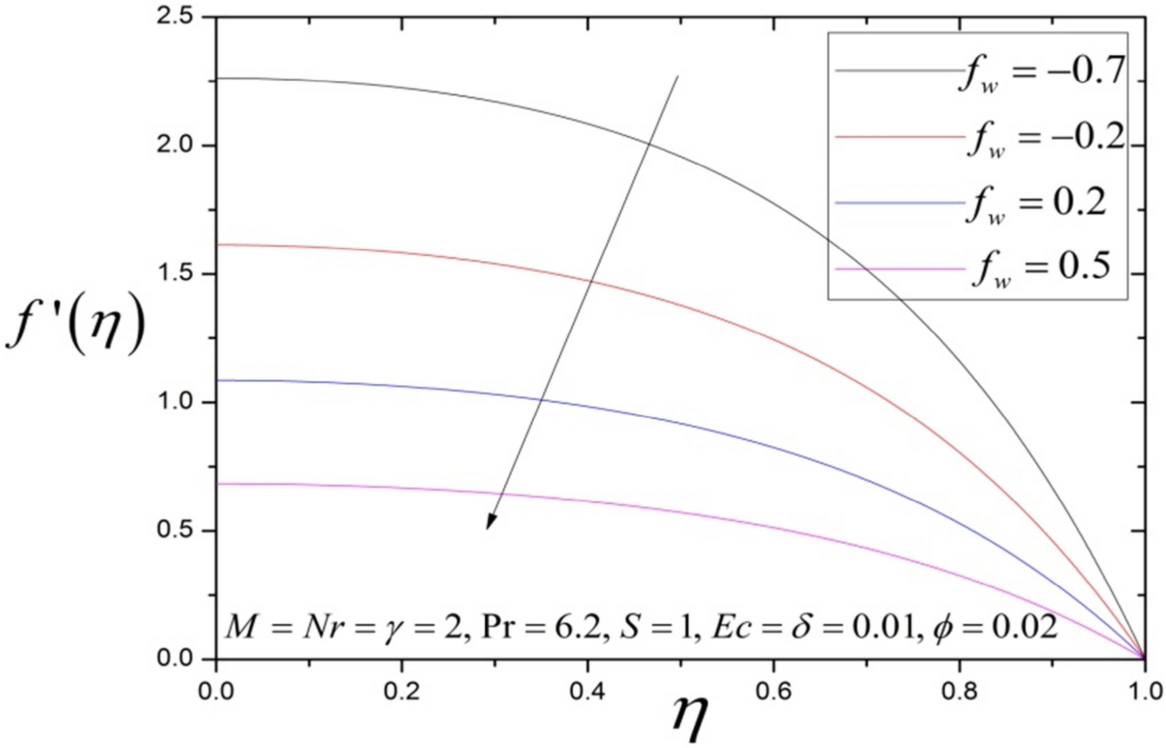

Figure 7. *Variation in velocity f'(η) due to several values of f_w.*

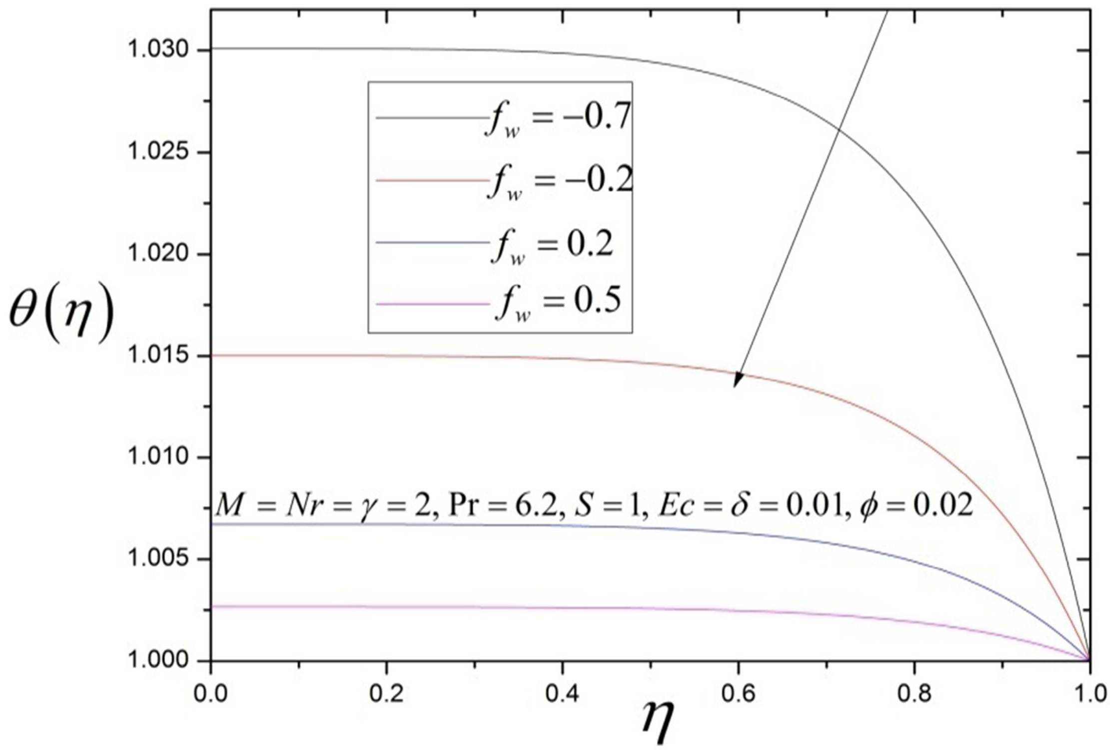

Figure 8. *Variation in temperature θ(η) due to several values of* f_w.

The variation in momentum boundary layer and thermal boundary layer profiles versus similarity variable η are represented in Figures 9 and 10 for three different value of nanoparticle volume fraction ϕ. It is noticeable in Figure 9 that on increasing in the values of volume of solid particle velocity boundary layer is decreased near the vicinity of the plates, while far from the surface of plates it increased. Figure 10 depicts that temperature of nanoparticle regularly declines with raise in volume of the solid particle, and due to this cause thickness of thermal boundary layer depreciates. According to Table 4 as increase in solid volume fraction, the values of $\left|-f''(0)\right|$ is reduced, while heat transfer rate is enhanced with elevate in volume fraction ϕ.

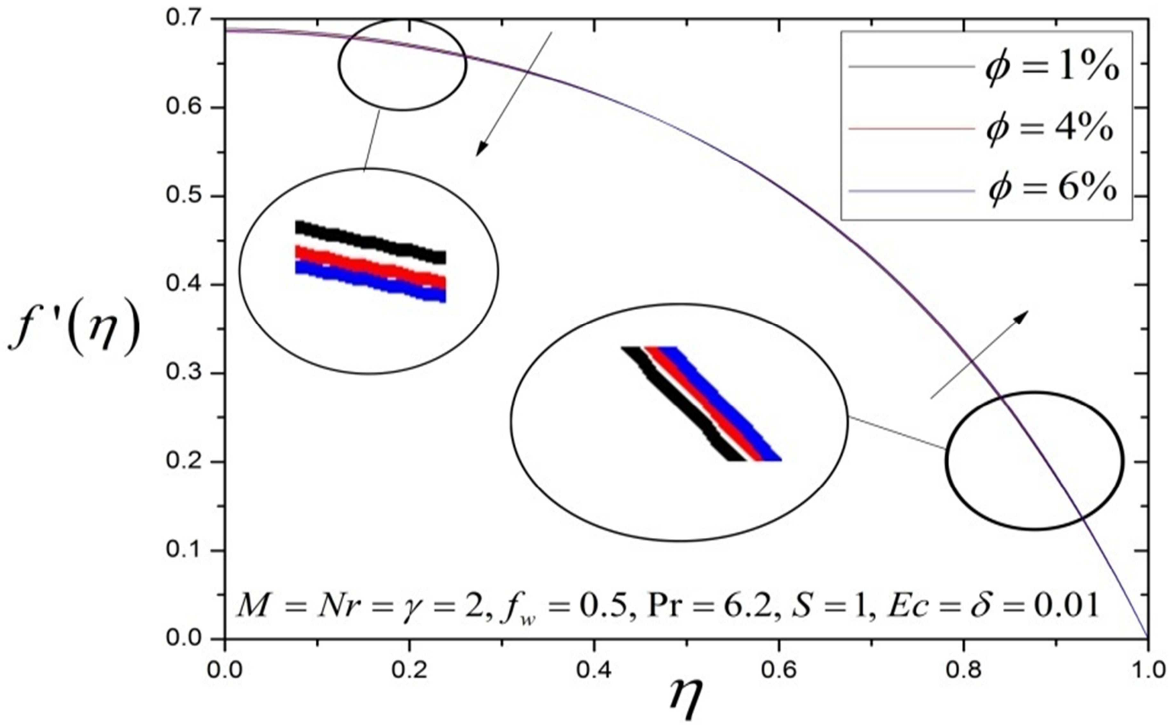

Figure 9. *Variation in velocity f'(η) due to several values of Φ.*

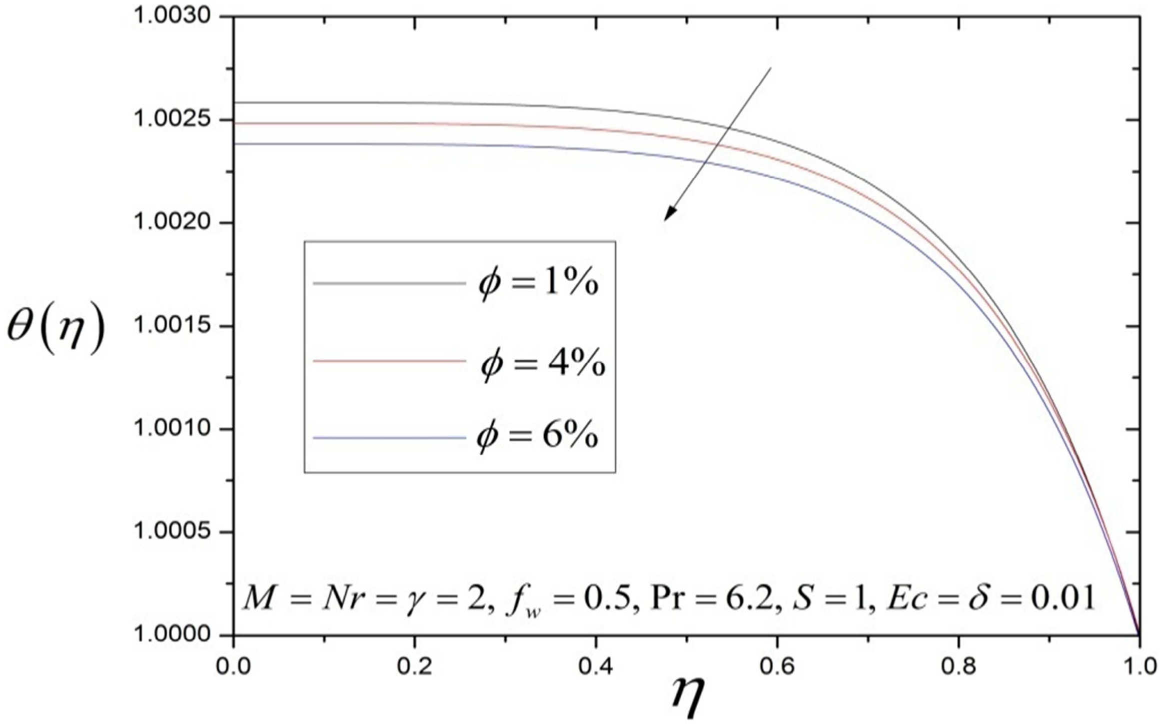

Figure 10. *Variation in temperature θ(η) due to several values of Φ.*

5. Conclusion

The impact of various governing parameters like thermal radiation parameter Nr, magnetic parameter M, porous medium parameter γ, suction/injection parameter f_w and the nanoparticle volume faction ϕ on flow and heat transfer of a squeezing unsteady nanofluid MHD flow between analogous plates in porous medium in the occurrence of thermal radiation and suction/injection taking water like regular fluid and Cu alike nanofluid particle was analyzed. The dimensionless velocity and temperature outlines have studied. It was concluded that on growing the value of suction/injection parameter f_w, both the velocity and temperature of nanoparticle significantly decreased, while temperature of nanoparticle decreases on mounting the values of the thermal radiation parameter. As increasing in magnetic parameter, the absolute value of skin friction $\left|-f''(0)\right|$ and Nusselt number $-\theta'(0)$ are augmented. The coefficient of heat transfer reduces on elevating the values of radiation parameter and volume concentration of nanoparticle.

References

[1] M. Azimi, R. Riazi, Heat transfer analysis of GO-water nanofluid flow between two parallel disks, Prop. Power Res. 4 (1) (2015) 23-30.

[2] A. Aziz, W. A. Khan, I. Pop, Free convection boundary layer flow past a horizontal flat plate embedded in porous medium filled by nanofluid containing gyrotactic microorganisms, Int. J. Therm. Sci. 56 (2012) 48-57.

[3] S. Das, A. S. Banu, R. N. Jana, O. D. Makinde, Entropy analysis on MHD pseudo-plastic nanofluid flow through a vertical porous channel with convective heating, Alexandria Eng. J. 54 (3) (2015) 325-337.

[4] G. Domairry, M. Hatami, Squeezing Cu–water nanofluid flow analysis between parallel plates by DTM-Padé Method, J. Mol. Liq. 193 (2014) 37-44.

[5] M. Fakour, D. D. Ganji, M. Abbasi, Scrutiny of underdeveloped nanofluid MHD flow and heat conduction in a channel with porous walls, Cas. Stud. Therm. Eng. 4 (2014) 202-214.

[6] T. Groşan, C. Revnic, I. Pop, D. B. Ingham, Free convection heat transfer in a square cavity filled with a porous medium saturated by a nanofluid, Int. J. Heat Mass Transf. 87 (2015) 36-41.

[7] A. K. Gupta, S. S. Ray, Numerical treatment for investigation of squeezing unsteady nanofluid flow between two parallel plates, Powd. Technol. 279 (2015) 282-289.

[8] B. K. Jha, B. Aina, A. T. Ajiya, MHD natural convection flow in a vertical parallel plate microchannel, Ain Shams Eng. J. 6 (1) (2015) 289-295.

[9] A. Khalid, I. Khan, A. Khan, S. Shafie, Unsteady MHD free convection flow of Casson fluid past over an oscillating vertical plate embedded in a porous medium, Eng. Sci. Technol. Int. J. 18 (3) (2015) 309-317.

[10] A. V. Kuznetsov, D. A. Nield, The Cheng–Minkowycz problem for natural convective boundary layer flow in a porous medium saturated by a nanofluid: a revised model, Int. J. Heat Mass Transf. 65 (2013) 682-685.

[11] M. Mustafa, T. Hayat, S. Obaidat, On heat and mass transfer in the unsteady squeezing flow between parallel plates, Meccan. 47 (7) (2012) 1581-1589.

[12] O. Pourmehran, M. Rahimi-Gorji, M. Gorji-Bandpy, D. D. Ganji, Analytical investigation of squeezing unsteady nanofluid flow between parallel plates by LSM and CM, Alexandria Eng. J. 54 (1) (2015) 17-26.

[13] M. Sheikholeslami, D. D. Ganji, Nanofluid flow and heat transfer between parallel plates considering Brownian motion using DTM, Comput. Meth. Appl. Mech. Eng. 283 (2015) 651-663.

[14] W. Ibrahim, B. Shankar, MHD boundary layer flow and heat transfer of a nanofluid past a permeable stretching sheet with velocity, thermal and solutal slip boundary conditions, Comput. Fluids 75 (2013) 1-10.

[15] A. K. Pandey, M. Kumar, Effect of Viscous dissipation and suction/injection on MHD nanofluid flow over a wedge with porous medium and slip, Alexandria Eng. J. 55 (2016) 3115–3123.

[16] A. K. Pandey, M. Kumar, Natural convection and thermal radiation influence on nanofluid flow over a stretching cylinder in a porous medium with viscous dissipation, Alexandria Eng. J. 56 (1) (2017) 55-62.

[17] M. Hatami, M. Khazayinejad, D. Jing, Forced convection of Al_2O_3–water nanofluid flow over a porous plate under the variable magnetic field effect, Int. J. Heat Mass Transf. 102 (2016) 622-630.

[18] M. Sheikholeslami, M. M. Rashidi, D. D. Ganji, Effect of non-uniform magnetic field on forced convection heat transfer of Fe_3O_4–water nanofluid, Comput. Meth. Appl. Mech. Eng. 294 (2015) 299-312.

[19] A Mahmoudi, I Mejri, M. A. Abbassi, A. Omri, Analysis of MHD natural convection in a nanofluid filled open cavity with non-uniform boundary condition in the presence of uniform heat generation/absorption, Powd. Technol. 269 (2015) 275-289.

[20] A. S. Dogonchi, K. Divsalar, D. D. Ganji, Flow and heat transfer of MHD nanofluid between parallel plates in the presence of thermal radiation, Comput. Meth. Appl. Mech. Eng. 310 (2016) 58-76.

[21] S. K. Nandy, T. R. Mahapatra, Effects of slip and heat generation/absorption on MHD stagnation flow of nanofluid past a stretching/shrinking surface with convective boundary conditions, Int. J. Heat Mass Transf. 64 (2013) 1091-1100.

[22] B. Jalilpour, S. Jafarmadar, D. D. Ganji, A. B. Shotorban, H. Taghavifar, Heat generation/absorption on MHD stagnation flow of nanofluid towards a porous stretching sheet with prescribed surface heat flux, J. Molec. Liq. 195 (2014) 194-204.

[23] D. Pal, G. Mandal, Hydromagnetic convective–radiative boundary layer flow of nanofluids induced by a non-linear vertical stretching/shrinking sheet with viscous–Ohmic dissipation, Powd. Technol. 279 (2015) 61-74.

[24] K. Vajravelu, K. V. Prasad, J. Lee, C. Lee, I. Pop, R. A. Van Gorder, Convective heat transfer in the flow of viscous Ag–water and Cu–water nanofluids over a stretching surface, Int. J. Therm. Sci. 50 (5) (2011) 843-851.

[25] A. Karimipour, A. D'Orazio, M. S. Shadloo, The effects of different nanoparticles of Al_2O_3 and Ag on the MHD nano fluid flow and heat transfer in a microchannel including slip velocity and temperature jump, Phys. E: Low-dim. Systems and Nanostructures 86 (2017) 146-153.

[26] A. Behrangzade, M. M. Heyhat, The effect of using nano-silver dispersed water based nanofluid as a passive method for energy efficiency enhancement in a plate heat exchanger, Appl. Therm. Eng. 102 (2016) 311-317.

[27] T. Hayat, T. Abbas, M. Ayub, M. Farooq, A. Alsaedi, Flow of nanofluid due to convectively heated Riga plate with variable thickness, J. Molec. Liq. 222 (2016) 854-862.

[28] A. R. Ahmadi, A. Zahmatkesh, M. Hatami, D. D. Ganji, A comprehensive analysis of the flow and heat transfer for a nanofluid over an unsteady stretching flat plate, Powd. Technol. 258 (2014) 125-133.

[29] M. M. Rashidi, M. Reza, S. Gupta, MHD stagnation point flow of micropolar nanofluid between parallel porous plates with uniform blowing, Powd. Technol. 301 (2016) 876-885.

[30] M. Sheikholeslami, D. D. Ganji, Heat transfer of Cu-water nanofluid flow between parallel plates. Powd. Technol. 235 (2013) 873-879.

[31] M. Sheikholeslami, M. M. Rashidi, D. M. Al Saad, F. Firouzi, H. B. Rokni, G. Domairry, Steady nanofluid flow between parallel plates considering thermophoresis and Brownian effects, J. King Saud Univ.-Sci. 28 (4) (2016) 380-389.

[32] B. Ganga, S. M. Y. Ansari, N. V. Ganesh, A. A. Hakeem, MHD radiative boundary layer flow of nanofluid past a vertical plate with internal heat generation/absorption, viscous and Ohmic dissipation effects, J. Nigerian Math. Soc. 34 (2) (2015) 181-194.

[33] N. A. M. Zin, I. Khan, S. Shafie, The impact silver nanoparticles on MHD free convection flow of Jeffrey fluid over an oscillating vertical plate embedded in a porous medium, J. Molec. Liq. 222 (2016) 138-150.

[34] M. A. Mansour, S. E. Ahmed, A numerical study on natural convection in porous media-filled an inclined triangular enclosure with heat sources using nanofluid in the presence of heat generation effect, Eng. Sci. Technol. Int. J. 18 (3) (2015) 485-495.

[35] A. K. Pandey, M. Kumar, Boundary layer flow and heat transfer analysis on Cu-water nanofluid flow over a stretching cylinder with slip, Alexandria Eng. J. 56 (4) (2017) 671-677.